JOWRM

Journal of Water Resources Management

Journal homepage: https://journal.water.gov.my

e-ISSN: 2811-3578

Towards Safer Spillways: A Hybrid Approach To Flow Induced Vibration Analysis And Structural Integrity Assessment

Nurul Husna Hassan[1,a], Mohd Hafiz Zawawi[2,b], Mohd Rashid Mohd Radzi[3,c], Ahmad Zhafran Ahmad Mazlan[4,d], Mohamad Aizat Abas[5,e], Mohd Remy Rozainy Mohd Arif Zainol[6,f]

[1,2] Department of Civil Engineering, Universiti Tenaga Nasional,
Jalan Kajang-Puchong, 43000 Kajang, Selangor, MALAYSIA

[3] Hydro Life Extension Program (HLEP), TNB Power Generation Division, Malaysia,
Jalan Bangsar, 59200 Kuala Lumpur, MALAYSIA

[4,5] School of Mechanical Engineering, Universiti Sains Malaysia,
14300 Nibong Tebal, Penang, MALAYSIA

[6] School of Civil Engineering, Universiti Sains Malaysia, Malaysia,
14300 Nibong Tebal, Penang, MALAYSIA

*Corresponding Author
Email: [a]nhh.husnahassangmail.com, [b]MHafiz@uniten.edu.my, [c]RashidMR@tnb.com.my, [d]zhafran@usm.my, [e]aizatabas@usm.my, [f]ceremy@usm.my,

Received 05 March 2025;
Accepted 19 November 2025;
Available online 27 December 2025

Abstract: Spillways play a crucial role in regulating water discharge from dams, ensuring structural safety and mitigating flood risks. This study investigates the flow-induced vibrations and structural integrity of the Kenyir Dam chute spillway using a hybrid approach combining numerical simulations and experimental validation. A fluid-structure interaction (FSI) model was developed to analyze hydraulic and structural parameters, including velocity, pressure, stress, and deformation, under varying water levels. The findings reveal that higher water levels significantly increase flow velocity and pressure, leading to greater stress and deformation, though still within safe operational limits. Modal and harmonic response analyses identified critical mode shapes and natural frequencies, highlighting potential vibration risks. Experimental validation using a scaled hydraulic model confirmed the accuracy of the numerical predictions, with a maximum discrepancy of 14.01%. The results provide valuable insights into spillway safety management, supporting predictive maintenance strategies and the optimization of spillway designs to prevent structural failures.

Keywords: Spillway safety, flow-induced vibration, fluid-structure interaction, numerical simulation, experimental validation.

1. Introduction

Dams play a crucial role in water resource management, flood control, irrigation, and hydroelectric power generation [1], [2]. These massive structures are designed to regulate river flow, ensuring water availability during dry seasons while mitigating flood risks during heavy rainfall. Dams can be categorized based on their construction materials and design, including embankment dams, concrete gravity dams, and arch dams. Despite their benefits, dams face several challenges, including structural integrity concerns, sedimentation, and environmental impacts [3], [4].

A critical component of any dam is the spillway, which facilitates the controlled release of excess water to prevent overtopping and potential failure. Spillways can be designed in various forms, such as ogee, chute, shaft, and siphon spillways, depending on site-specific hydraulic and topographical considerations. Among these, chute spillways are commonly used for high-velocity flows, effectively directing water downstream while minimizing erosion and structural damage [5], [6].

Kenyir Dam, also known as the Sultan Mahmud Power Station is a hydroelectric dam located in Terengganu, Malaysia. The dam consists of four major components which are the spillway, dam crest, office complex, and power station.

**Corresponding author: nhh.husnahassangmail.com*

Kenyir Dam chute spillway is an uncontrolled chute spillway, meaning it lacks gates for water regulation. Its steep design enables it to handle high-velocity supercritical flow, efficiently directing flood discharge downstream. The main materials include concrete and granite, with the latter serving as an energy dissipator at the lower section. The spillway is particularly vulnerable to flow-induced vibrations due to high-velocity water discharge. Despite regular inspections, the risks associated with structural fatigue, material degradation, and vibrational resonance necessitate a robust analytical approach.

While essential for flood management, excessive spillway discharge poses risks, including erosion, structural degradation, and flow-induced vibrations. The insecurity of the dam structure may be affected due to vibration uncertainties induced by internal and external sources, including discharge water, hydropower machineries, and other related factors and it is a major concern as uncontrolled vibrations may weaken the dam over time, increasing the risk of failure [7], [8].

The absence of energy dissipators due to erosion further exacerbates the situation, as observed in the Oroville Dam failure in California (2017), where high-velocity discharge dislodged granite boulders, leading to extensive erosion and operational failures. Despite scheduled inspections and maintenance, any failures may go undetected due to the spillway scale [9]. Additionally, resonance effects are a potential threat if the operational frequency of the spillway matches its natural frequency, vibrations could amplify and significantly increasing stress on the structure [10].

This study investigates the correlation between water discharge levels and vibration characteristics using FSI analysis and experimental validation. The objectives include determining hydraulic and structural parameters such as pressure, velocity, stress, and deformation, as well as identifying the natural and operational frequencies of the spillway. A validated numerical-experimental framework will be established to analyze flow-induced vibrations in chute spillways. This study contributes to spillway safety management by offering predictive insights into structural integrity and providing a tool for preventive maintenance planning.

1.1 Fluid-Structure Interaction

Fluid-Structure Interaction (FSI) is a multidisciplinary approach that examines the interaction between fluid flow and structural components [11]. In dam spillway structures, FSI plays a critical role in evaluating the dynamic response of the system to high-velocity water flow. The coupling of hydrodynamic forces with structural integrity analysis ensures a comprehensive assessment of how the spillway withstands operational conditions and potential failure scenarios [12]. As depicted in Fig. 1, the interaction between the fluid and the structure is interdependent, where the motion or deformation of one entity influences the other, and conversely. These interactions are termed as one-way. In cases where the interface sequentially transfers data to both sides, it is referred to as two-way interaction [13], [14].

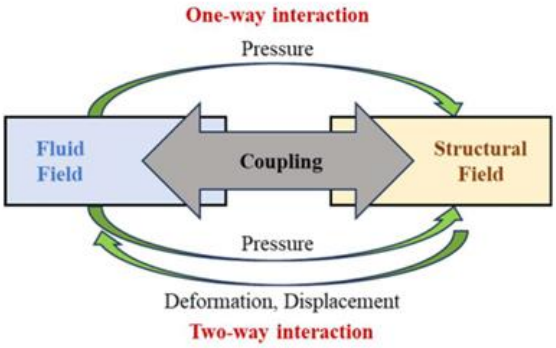

Fig. 1 – Concept of fluid-structure interaction

Twarog has investigated the structural behavior of the Niedow Dam spillway in Poland using Flow-3D software to analyze the effects of water discharge loads. The study aimed to visualize displacements, deformations, and stress distributions within the spillway under specific operating conditions [15]. Through FSI analysis, the research focused on key concrete components, demonstrating the capability of advanced computational methods in detecting regions experiencing variable stress levels. This highlights the crucial role of modern numerical modeling in evaluating the structural integrity and performance of hydraulic structures [16].

1.2 Flow-Induced Vibration

Flow-induced vibration (FIV) analysis is essential in assessing the structural response of dam, specifically on spillways subjected to high-velocity water flow [17], [18]. When water flows rapidly over the spillway surface, it generates fluctuating pressure forces that interact with the structural components, potentially leading to vibration-related issues. FIV occurs due to various mechanisms, including vortex shedding, turbulent buffeting, and fluid-elastic instability [19].

Analyzing the FIV behavior of spillway structures involves identifying the natural frequencies and mode shapes of the spillway to determine whether resonance conditions exist. If the spillway's operating frequency aligns with its natural frequency, significant amplification of vibrations can occur, increasing stress levels and leading to material fatigue. Computational methods, such as modal and harmonic analysis, help evaluate these parameters and ensure that the structural integrity of the spillway remains intact under operational conditions [19], [20].

In hydraulic engineering projects involving overflow gravity dams, such as the Three Gorges and Xiangjiaba dams, spillway guide walls are constructed to channel and stabilize water flow. Due to their larger scale compared to other lightweight hydraulic structures like hydraulic gates and gate piers, spillway guide walls are more susceptible to FIV damage, which can be more severe and challenging to repair. Several reported cases of such damage include Texarkana, Trinity, Wan'an, and Wujiangdu [21]. A study by Lian et al. has identified fatigue cracking as the most common failure mode of guide walls. Prolonged exposure to fluctuating flow conditions subjects the structure to varying pressures on both sides, leading to vibrations that can cause cracks near the base. Over time, this progressive deterioration may result in structural failure and eventual collapse of the guide wall [22].

By integrating FIV analysis with FSI simulations, engineers can identify vulnerable regions within the spillway structure and develop mitigation strategies such as optimizing spillway geometry, incorporating energy dissipators or modifying construction materials to enhance damping properties [23].

1.3 Hydraulic Physical Model

A hydraulic physical model is an essential tool in spillway research, allowing engineers to simulate real-world hydraulic conditions on a smaller scale [24], [25]. These models are typically developed using Froude similarity principles, ensuring accurate replication of flow patterns, velocity distributions, and energy dissipation mechanisms. By constructing a scaled down physical model, researchers can analyze spillway performance under different discharge conditions, evaluate flow behavior, and identify potential structural vulnerabilities [26].

Physical modeling provides valuable insights into complex hydraulic phenomena such as flow turbulence, aeration effects, and energy dissipation efficiency. It also serves as a crucial validation tool for numerical simulations, enabling direct comparisons between experimental results and computational predictions. In spillway studies, hydraulic physical models are used to assess the impact of water discharge on structural stability, identify regions of high stress concentration, and optimize spillway geometry for improved performance [27], [28].

2. Methodolgy

This section introduces the research methodology aimed at fulfilling the objectives of the study. The research methodology adopted in the current research work is to assess the structural reliability and integrity of Kenyir Dam spillway which had integrated various numerical and experimental.

2.1 Development of Three-Dimensional Model and Boundary Condition

The three-dimensional (3D) model of the Kenyir spillway was developed using SolidWorks software, incorporating topographical data, as-built drawings and material characterization results. The spillway structure was modeled as a single entity to ensure topological consistency while the surrounding hydraulic environment was replicated to enable accurate FSI simulations. Fig. 2 depicted the 3D model drawing of Kenyir spillway that contains two main materials which are concrete and granite.

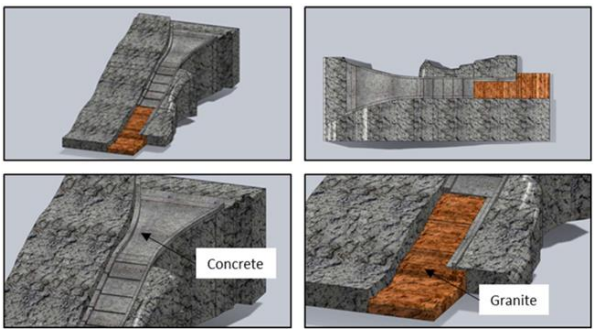

Fig. 2 - 3D model drawing of Kenyir spillway

For boundary conditions, the spillway's base was fixed to represent the foundation, while three-dimensional excitation forces were applied along the x, y, and z axes. The upstream fluid domain encompassed four water levels which are 146 m, 148 m, 150 m, and 152 m to simulate different operational conditions.

The upper bound of 152 m was selected because it corresponds to the Probable Maximum Flood (PMF) level for Kenyir Dam. Historical records indicate that actual spilling water levels have never exceeded 149 m, making 152 m a conservative estimate that captures the most extreme natural flood conditions anticipated [29]. This selection aligns with regulatory norms where PMF is used as the design threshold for dam safety evaluations [29]. Furthermore, the study aims to assess structural integrity under realistic but worst-case flood scenarios using a fluid-structure interaction (FSI) framework. Extreme cases such as seismic induced overtopping or cascading failures are outside the scope of this analysis and would require a distinct risk-based methodology. By focusing on PMF scenarios, the study ensures analytical relevance while maintaining computational feasibility [29], [30].

A periodic boundary condition as shown in Fig. 3 was applied to ensure continuous water flow, while a pressure outlet was assigned to represent water exiting into the downstream environment. Setting the boundary conditions for both the fluid and structure models, along with their respective degrees of freedom, is essential prior to conducting FSI and modal analysis. The study conducted by Radzi et al. demonstrates that the structural response varies depending on the location where pressure is applied [31]. This prove that a proper boundary condition will produce a better and more realistic result.

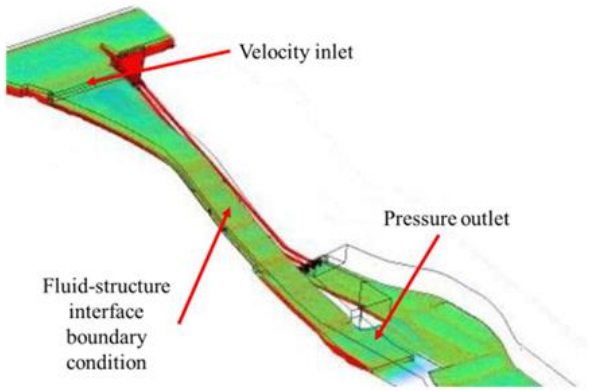

Fig. 3 - Boundary condition setup for FSI simulation

2.2 Meshing Sensitivity Analysis

A grid-independence test was conducted to minimize discretization error and ensure that the simulation results are not significantly influenced by mesh configuration. This test is essential prior to executing the full simulation as it verifies that variations in mesh type and element size do not affect the accuracy of results, particularly in critical regions of the model [32, 33].

Three different mesh models were developed and each utilizing distinct mesh types, grid elements and node densities. The objective was to confirm that the simulation outcomes

remain consistent regardless of mesh refinement. While finer meshes offer greater accuracy, they demand higher computational resources, whereas coarser meshes may compromise reliability.

Maximum stress for spillway concrete material was selected as the key comparison parameter among the models. The results summarized in Table 1 show that Mesh Model 2 produced a very low discretization error of just 0.03%, making it the optimal choice. This hexahedral mesh configuration effectively balances computational efficiency with solution precision.

Through multiple simulation runs with different mesh configurations, the goal is to discern the sensitivity of the solution to changes in the mesh. This analytical approach aids in optimizing mesh parameters to find the right balance between computational efficiency and solution accuracy [32].

Table 1 - Mesh independence test model

Mesh model	1	2	3
No. of elements	16925	55368	82573
No. of nodes	21042	82371	153702
Maximum stress (MPa)	4.11	7.23	7.27
Discretization error (%)	3.13	0.03	0.03

Meanwhile, Table 2 shows the comparison between the mesh sizes, number of elements and maximum velocity for the fluid domain of the spillway section. From the analysis, the mesh model with curvature and proximity minimum size of 0.07 m resulted in the least number of elements of 94437 elements and highest maximum velocity of 3.289 m/s.

Theoretically, a higher number of elements will produce more accurate result since more nodes being shared between elements. This means more time is required to solve the respective simulation and causes a higher computational cost.

Table 2 - Comparison of meshing type and the natural frequency of fluid section

Mesh size (m)	Number of elements	Maximum velocity (m/s)
0.05	184040	1.417
0.055	147972	1.416
0.06	124126	1.441
0.065	102952	2.416
0.07	94437	3.289

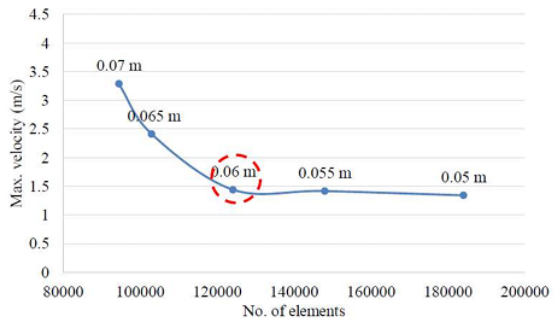

Fig. 4 - Optimum mesh size for spillway fluid section

Based on the graph of meshing sensitivity analysis in Fig. 4, the mesh model with 0.06 m element size is the most optimized mesh size since the maximum velocity started to saturate at this value and further analysis with smaller mesh size will not affect the results significantly. Fig. 5 depicted the optimum meshed body of spillway fluid section for mesh size of 0.06 m.

Fig. 5 - Optimum mesh size for spillway fluid section

For structural section meshing, the number of elements for the mesh with 1.0 m is the highest which is 1883854 elements, followed by 5.0 m and 10.0 m sizes with 43955 elements and 14950 elements respectively. For this study, due to the computational capability, the 5.0 m element size is chosen for the structure since it is suitable for the computational capability and reliable for the simulation. In addition, the first mode shape for both 1.0 m and 5.0 m element sizes are the same. Table 3 shows the comparison between element size and the natural frequency of the structural section and Fig. 6 depicted the optimum mode shape of spillway structural section for mesh size of 5.0 m.

Table 2 - Comparison between element size and the natural frequency of the structural section

Mesh size (m)	Number of elements	First natural frequency (Hz)
1.0	1883854	20.11
5.0	43955	20.34
10.0	14950	21.13

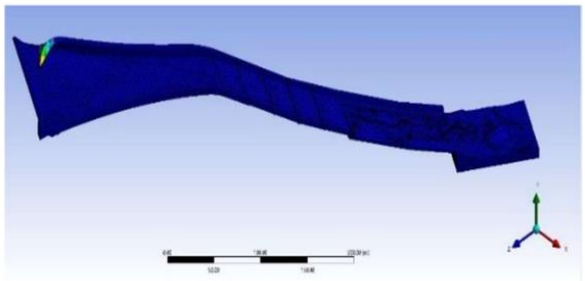

Fig. 6 - Optimum mesh size for spillway structural section

2.3 Fluid-Structure Interaction Analysis

In this study, the fluid domain is regarded as an incompressible fluid that characterized by parameters such as acceleration due to gravity and the characteristic length [33]. To perform the fluid simulation study, an approach involving the solution of partial differential equations derived from the Navier-Stokes equation is employed. The general Navier-Stokes equations can be represented as follows.

$$\frac{\partial}{\partial t}\left(\rho\vec{V}\right) + \nabla\cdot\left(\rho\vec{V}\vec{V}\right) = -\nabla p + \nabla\cdot(\tau) + \rho\vec{f} \quad (1)$$

Where, ρ is the fluid density, $\vec{V}$ is the fluid velocity vector, τ is the stress tensor and $\vec{f}$ is the external body force. Utilizing the basic principles of mechanics on a fluid gives equations governing the behavior [34]. Despite alterations in fluid volume and element shape during motion, its mass remains constant due to a consistent rate of mass change, conserving mass as it flows. The simulation aims to exert pressure on the spillway. Thus, the equation is coupled with mass and momentum equation without changing the simulation results.

The inclusion of the stress tensor is essential as it arises from fluid motion in a dynamic fluid, describing internal forces and hydrostatic pressure. To address the FSI problem involving a solid structure capable of altering the surrounding or internal fluid flow, various physical disciplines, laws, and equations must be included to allow the implementation of a full two way coupling [35]. This is achieved by integrating two solvers which are ANSYS Fluent for fluid simulation and ANSYS Transient Structural for structure simulation. Due to the complexity, the two-way coupled FSI simulation can provide desired results with enhanced accuracy [36].

2.4 **Flow-Induced Vibration Analysis**

ANSYS software is utilized to conduct modal analysis, which examines the structural dynamic behaviour of the spillway and identifies vibration characteristics such as mode shapes and natural frequencies. In the context of resilient movement in a damped system, the discrete component can be represented by the following linear differential equation.

$$[M]\{\ddot{x}(t)\} + [C]\{\dot{x}(t)\} + [K]\{x(t)\} = \{F(t)\} \quad (2)$$

Where, $[M]$ represents the mass matrix, $[C]$ is the damping matrix, $[K]$ is the stiffness matrix, $\{\ddot{x}(t)\}$ is the acceleration vector, $\{\dot{x}(t)\}$ is the velocity vector, $\{x(t)\}$ is the displacement vector and $\{F(t)\}$ represents the force vector.

In this study, firstly, the CAD file of spillway structure from the SolidWorks software is imported to the ANSYS software. Subsequently, the materials comprising the structure, namely concrete and granite, are allocated based on the corresponding area of the spillway section.

Harmonic response analysis involves loading with either harmonic or frequency-response characteristics, utilizing a single excitation frequency. The essential parameters for this analysis include Young's Modulus, Poisson's ratio, and mass density. The peak response in the harmonic analysis aligns with the natural frequencies of the structure [37]. The structure response over a frequency range can be calculated using harmonic analysis and the result obtained is used to plot the amplitude versus frequency graph with valuable dynamic characteristic information. ANSYS Harmonic can be used to simulate structural response under forced vibration and efficiently extract the forced excitation amplitude deflection of the structure [38].

The dynamic load is applied at different frequency to observe the relationship between amplitude and frequency in a steady-state response. The harmonic response function can be defined as follows.

$$([K] + i\omega[C] - \omega^2[M])(\{X_1\} + i\{X_2\}) = \{F_1\} + i\{F_2\} \quad (3)$$

Where, $\{F1\}$ is the real part of excitation force, $\{F2\}$ is the imaginary part of excitation force, i is the imaginary unit, ω is the excitation frequency, $\{X1\}$ is the real part of displacement amplitude and $\{X2\}$ is the imaginary part of displacement amplitude. Before conducting harmonic response analysis, the harmonic block is interconnected with the modal block in ANSYS software to investigate the specific responsive effects of the components [39].

2.5 **Experimental Validation**

The 1:50 scale hydraulic model was subjected to flow tests, with velocity measurements and vibration responses recorded to validate the numerical results. The validation in terms of water flow velocity has been conducted for both simulation and experimental physical models. Three location points have been selected to measure the velocity which are labelled as Point A, Point B and Point C as depicted in Fig. 7.

Point A marks the spillway inlet, Point B denotes the concrete section before the granite, and Point C represents the granite section before the scoured pool or the spillway outlet. The water flow velocity measurement for the spillway physical model has been conducted using velocity meter.

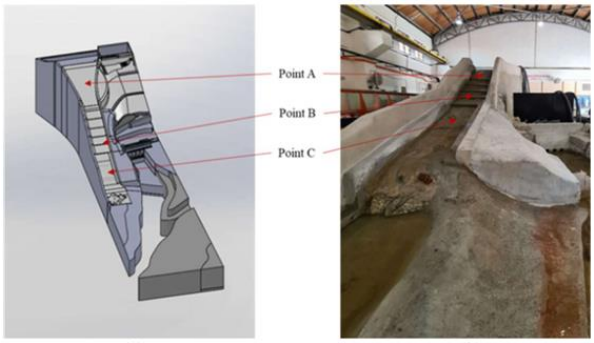

Fig. 7 - Location points of water flow velocity measurement for (a) simulation and (b) experiment at the spillway physical model

EMA is an experimental method in structural vibration analysis that employed to determine the parameters such as the natural frequencies, mode shapes, and damping ratio [40]. EMA results are then can be compared with the simulation for the validation purpose [41], [42]. Fig. 8 shows the points of the measurement and instrumentation used to conduct the EMA.

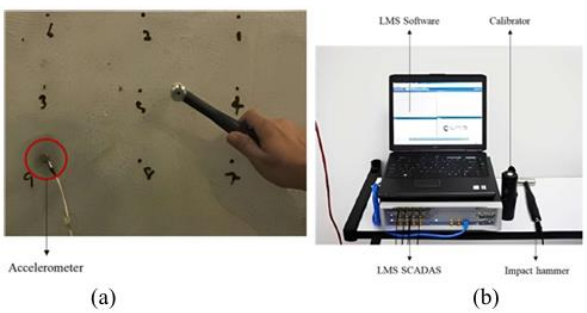

Fig. 8 - (a) Measurement points and (b) instrumentation for EMA

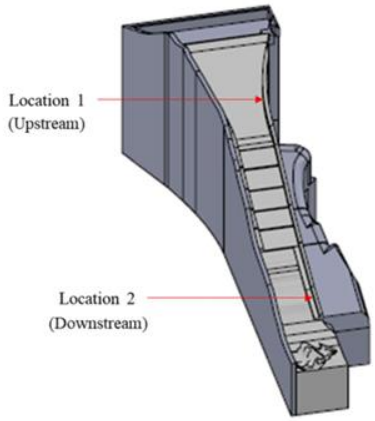

Fig. 9 - Measurement location at spillway physical model

Various tools and equipment are utilized including LMS software, LMS SCADAS, a calibrator, an impact hammer, and an accelerometer for performing EMA. Hammer impact testing method is used where the impact hammer is knocked from one point to another for all 9 points while the accelerometer is remains fixed at single point. The force applied by the impact hammer is acted as input and the accelerometer will record the output acceleration. The measurement locations at the spillway upstream and downstream named as Location 1 and Location 2 for the EMA measurement are depicted in Fig. 9.

Operational deflection shape (ODS) experiment is an experimental procedure to determine the spillway structure deflection shapes and operating frequency during the water spilling. The instrumentation involved in this experiment are two accelerometers, LMS SCADAS and LMS software. Two accelerometers which act as reference and output vibration are attached to the spillway structure to measure the operating frequency. One of the accelerometers will be moved from one point to another to get the measurement results for all 9 points.

3. Results And Discussion

3.1 Fluid-Structure Interaction Analysis

Water levels of 146 m, 148 m, 150 m, and 152 m were selected to investigate the impact of the spillway structure free surface water level on velocity and pressure. The 152 m water level is considered the worst-case scenario in this study based on the PMF of Kenyir Dam and the recorded water spilling level never exceeds 149 m.

For the inlet water phase, a volume fraction of 1 was set under the multiphase section. Water volume fraction is multiphase flow systems to represent the proportion of water in a mixture of different phases which in this study are water and air [3]. Fig. 10 to Fig. 13 depict the free surface water level of the spillway for each water level, respectively. These free surface water levels were determined based on observed data. The average water volume fraction for 146 m water level as shown in Fig. 10 was depicted at 0.1, while the average water volume fraction increases to 0.2, 0.3 and 0.4 for 148 m, 150 m and 152 m water level respectively accelerating with the water levels as shown in Fig. 11 to Fig. 13.

Fig. 14 depicted the spillway structure cross section that consists of four aerators that served to reduce the velocity along the spillway. Probabilistic calculations by Moghaddam et al. suggest that installing the first aerator alone certainly not guarantee the spillway safety. Post the second aerator installation, 7% failure probability, emphasizing the need for caution was calculated. To prevent discharge-related failures, a third aerator is added at the chute spillway beginning [43].

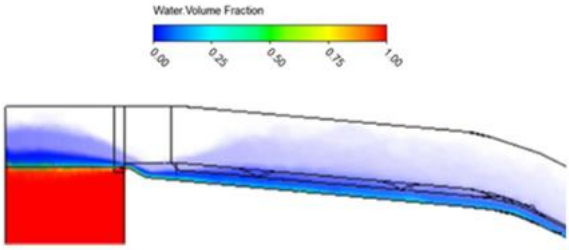

Fig. 10 - Free surface water level of spillway at 146 m

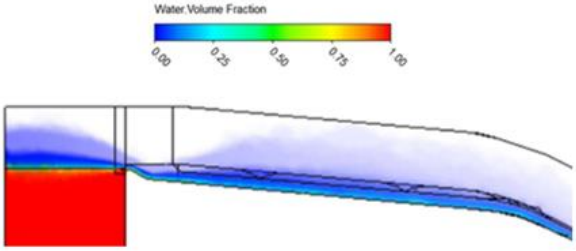

Fig. 11 - Free surface water level of spillway at 148 m

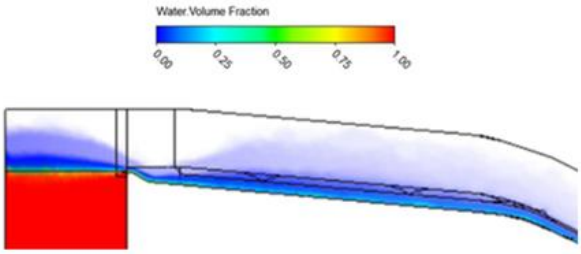

Fig. 12 - Free surface water level of spillway at 150 m

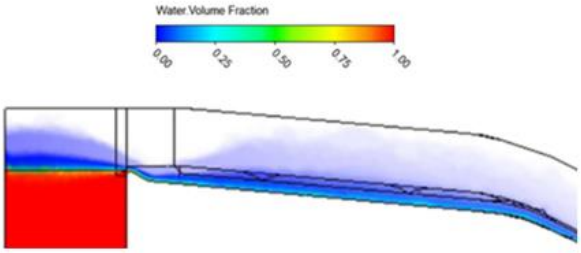

Fig. 13 - Free surface water level of spillway at 152 m

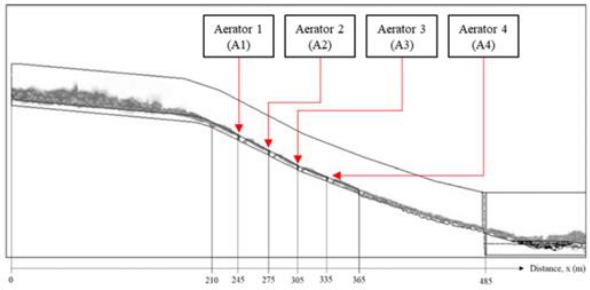

Fig. 14 - Location of the reference distance

Fig. 15 to Fig. 18 depict the flow velocity contours for the spillway flows at four water levels. The mean water velocity for 146 m, 148 m, 150 m and 152 m water levels through the spillway structure are 16 m/s, 24 m/s, 29 m/s and 36 m/s respectively. Due to the gravity, the flow velocity gradually rises as it moves towards the downstream section. It was observed that the average flow velocity increases in proportion to the water level. This is due to the increases in the discharge rate of the spillway flow as the water level increases. The highest velocity region for 146 m, 148 m, 150 m and 152 m was observed at the downstream spillway surface which are 40 m/s, 48 m/s, 51 m/s and 52 m/s respectively.

The findings reveal that the highest velocity among the aerators was recorded at Aerator 2 for water levels of 148 m, 150 m and 152 m measuring 26.8 m/s, 32.8 m/s and 42.9 m/s respectively. Unstable flow can lead to oscillations and uneven pressure distribution and introduction of air can produce stagnation pressure. Therefore, aerator can stabilize the flow, making it more uniform and reducing the risk of flow separation and turbulence that can cause structural problems [44], [45]. Fig. 19 shows the mean velocity on the spillway structure at different water level and it indicates the highest mean velocity is at water level of 152 m which is 36 m/s.

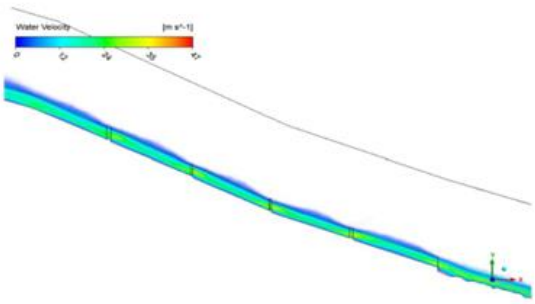

Fig. 15 - Aerator velocity contour at 146 m water level

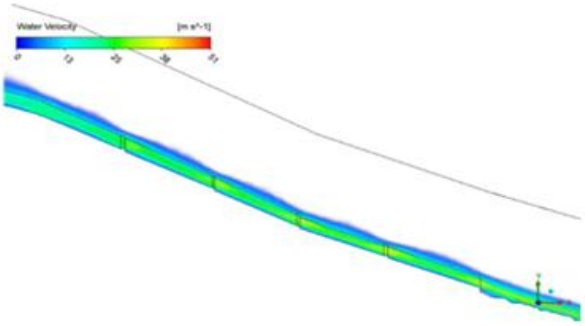

Fig. 16 - Aerator velocity contour at 148 m water level

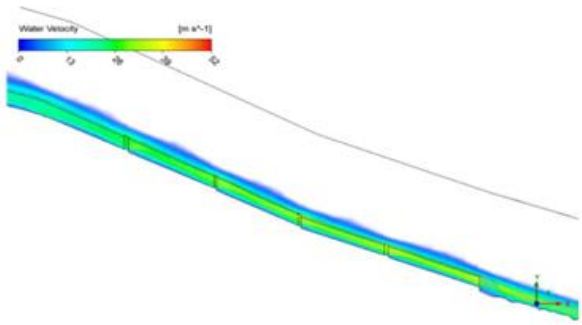

Fig. 17 - Aerator velocity contour at 150 m water level

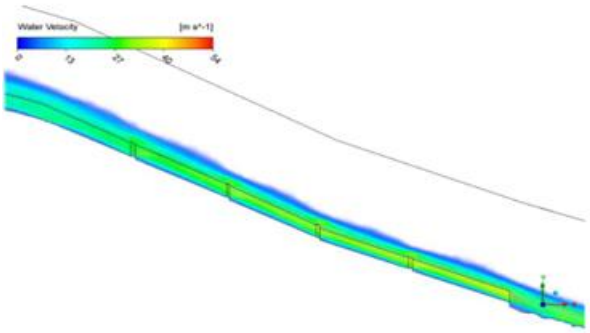

Fig. 18 - Aerator velocity contour at 152 m water level

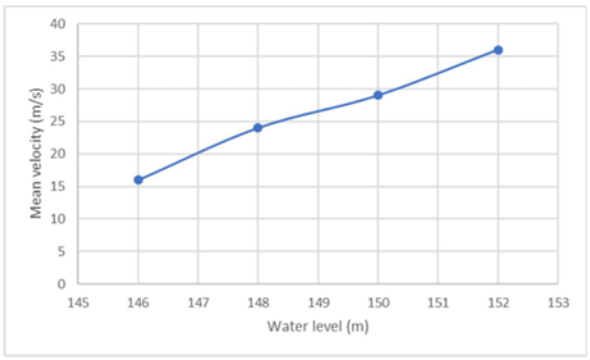

Fig. 19 - Plot of mean velocity against water level

As the manipulation of the water levels will exert different forces on the spillway structure, it could induce excessive vibration on the spillway structure. Fig. 20 to Fig. 23 depict the vibration excitation source in terms of the water pressure counter on the central plane. In general, the pressure will be increased as the water level increases [46]. This will lead to highvelocity water flows from the upstream to the downstream region in significant deflection, vibration and stress on the spillway.

However, it is able to endure high pressure due to the proper structure design [47]. The mean water pressure for 146 m, 148 m, 150 m and 152 m water levels through the spillway structure observed are 37 kPa, 67 kPa, 79 kPa and 145 kPa respectively. In the case of a non-viscous flow under steady conditions, Bernoulli's principle dictates that the total energy, comprising kinetic energy, potential energy, and pressure energy remains fixed. Consequently, as velocity increases, the pressure at that particular section decreases to uphold the overall energy constancy [48]. Fig. 24 shows the mean

pressure on the spillway structure at different water level and it indicates the highest mean pressure is at water level of 152 m which is 145 kPa.

Kenyir spillway consists of four aerators assuredly the study as the pressure at the Aerator 2 to Aerator 4 give significant difference pressure values. It can be observed in Table 3 that velocity water increases with increased discharge rate. As the discharge rate increases, the tangential velocity of the flow also increases resulting in an increase in centrifugal force on the water, thereby produces high velocity as shown in Fig. 25.

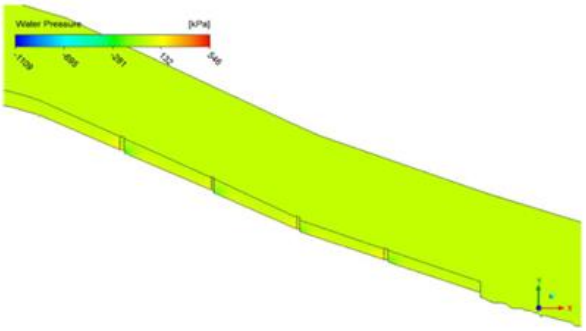

Fig. 20 - Aerator pressure contour at 146 m water level

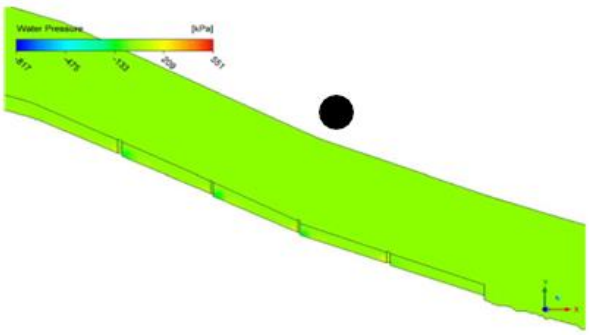

Fig. 21 - Aerator pressure contour at 146 m water level

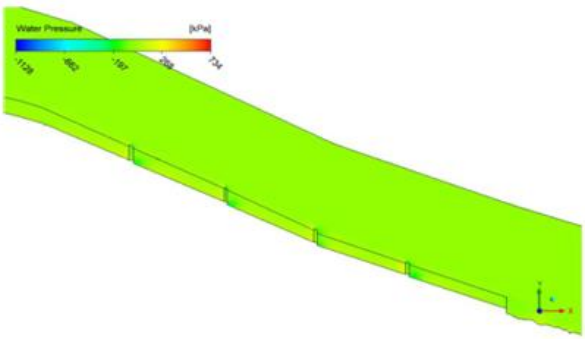

Fig. 22 - Aerator pressure contour at 150 m water level

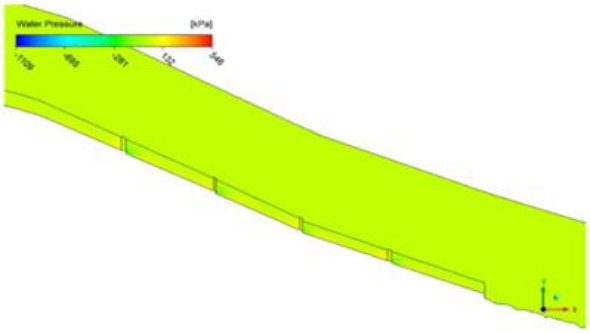

Fig. 23 - Aerator pressure contour at 152 m water level

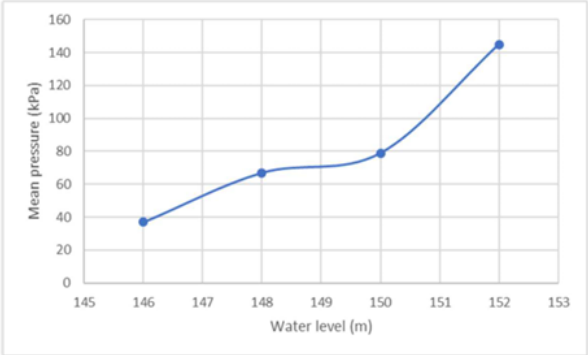

Fig. 24 - Plot of mean velocity against water level

Table 3 - Average velocity along the spillway for different water level

	Average velocity along the spillway (m/s)			
x (m)	**146**	**148**	**150**	**152**
0	2.4	4.7	5.6	6.1
210	8.0	14.7	17.2	24.8
245 (A1)	19.1	24.8	31.5	39.4
275 (A2)	14.5	26.8	32.8	42.9
305 (A3)	13.8	22.5	27.7	37.7
335 (A4)	14.2	23.6	30.6	39.8
365	16.0	26.7	32.4	41.6
485	40.0	48.0	51.0	52.0

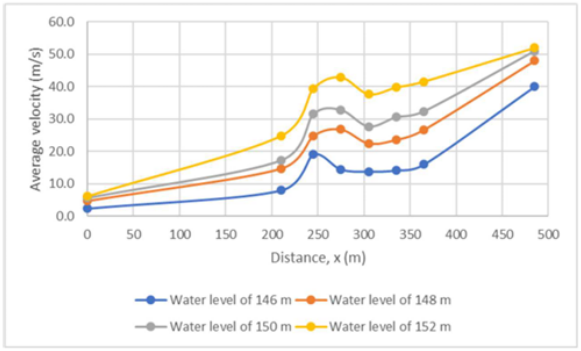

Fig. 25 - Plot of average velocity along the spillway for different water level

Fig. 26 to Fig. 29 show the stress contour for the spillway section at the four water levels respectively for structural part. This stress value is considerably safe for the structure since it is well below the allowable maximum compressive strength of granite which is 49.3 MPa. Meanwhile, for the stress of the concrete area, the value is slightly increased to 2 MPa as depicted in blue contour but no structural failure is expected. This is the most concerning water level if the water level is above this maximum level.

A study by Asgarzade et al. also investigated the worst-case scenario for dam wall failure involving the overtopping scenario with various hydraulic jumps [49]. Nevertheless, sustained interaction with water against the granite will eventually lead to a scouring effect over time [50]. Fig. 30 shows the maximum stress on the spillway structure at different water level and it indicates the highest maximum stress is at water level of 152 m which is 2.081 MPa.

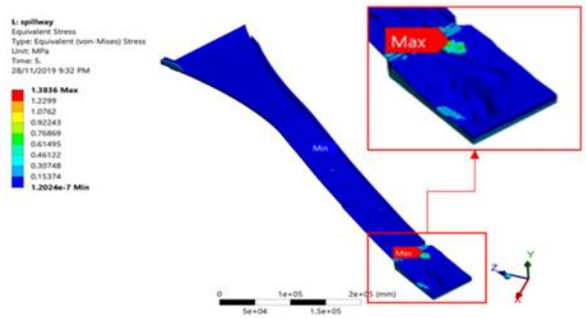

Fig. 26 - Stress contour at 146 m water level

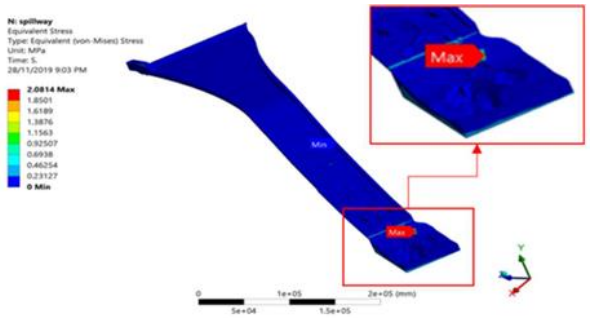

Fig. 27 - Stress contour at 148 m water level

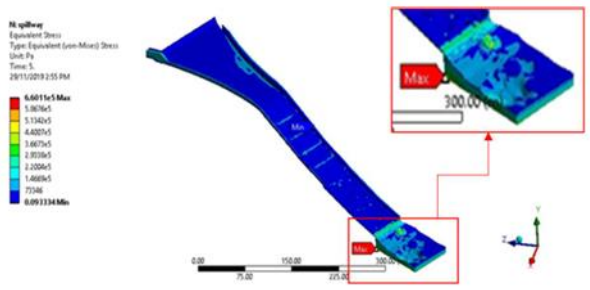

Fig. 28 - Stress contour at 150 m water level

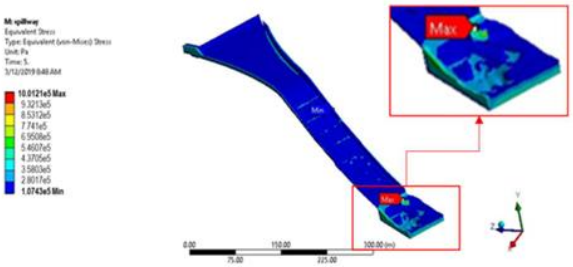

Fig. 29 - Stress contour at 152 m water level

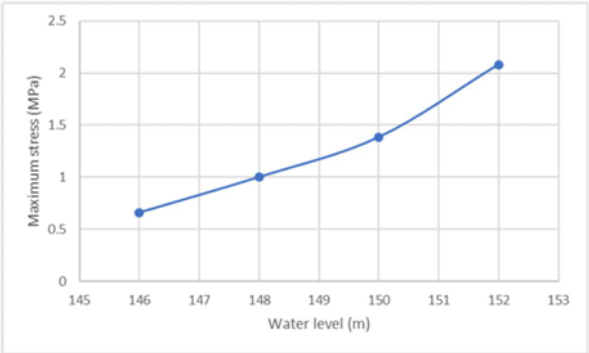

Fig. 30 - Plot of maximum stress against water level

During the water spills, the highest deformation is remarked at the end of the granite structure of the spillway downstream region which performs as an energy dissipater. Fig. 31 and Fig. 34 illustrated the deformation and stress contour for the spillway section at the four water levels respectively. The highest maximum deformation and stress occurred as a result of highwater velocity and pressure extending from the upstream to the downstream region at a water level of 152 m.

According to a study by Minmahddun and Ngii, the deformation of the structure increased as a result of elevated hydrostatic pressure on the upstream surface of the dam with the rise in reservoir water level [51]. Another study by Li et al. shows that the observed dam body deformation and stress distribution values were normal and lower than the design values [52]. Therefore, it is important to carry out condition monitoring to ensure the dam is in a safe condition during normal operation. Fig. 35 shows the maximum deformation against water level and it indicates the maximum deformation is at water level of 152 m which is 0.031 m.

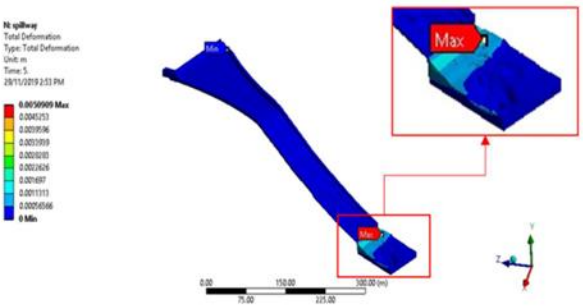

Fig. 31 - Deformation contour at 146 m water level

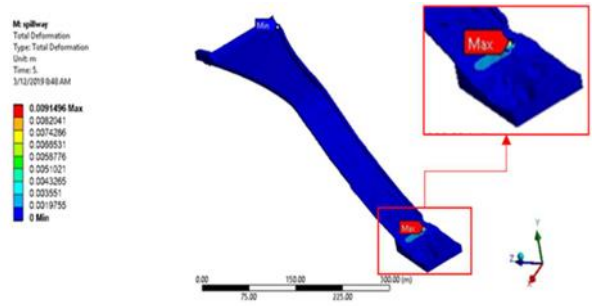

Fig. 32 - Deformation contour at 148 m water level

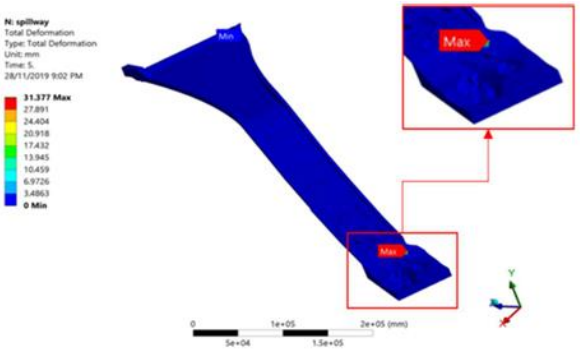

Fig. 33 - Deformation contour at 150 m water level

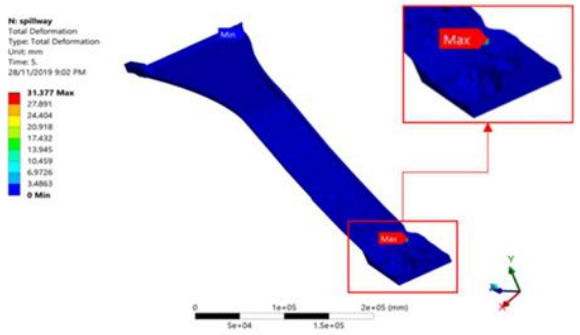

Fig. 34 - Deformation contour at 152 m water level

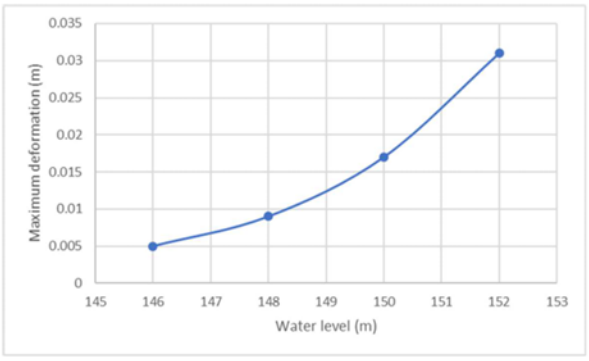

Fig. 35 - Plot of maximum stress against water level

The operation condition of the spillway is only dependent on the spilling water levels. Based on Table 4, the velocity, pressure, stress and deformation are accelerating with the water level and all of the stress values are below the allowable compressive strength.

Table 4 - Summary of overall FSI data analysis

Water level (m)	Mean velocity (m/s)	Mean pressure (kPa)	Max stress (MPa)	Max deformation (m)
146	16	37	0.660	0.005
148	24	67	1.001	0.009
150	29	79	1.384	0.017
152	36	145	2.081	0.031

3.2 Flow-Induced Vibration Analysis

This section presents the outcomes of modal and harmonic response analyses. Modal analysis is performed to determine the mode shapes, natural frequencies and normalised deflection and FRF graph of the spillway structure and then been compared with the results of ODS and operating frequencies at different levels of water spilling. There are total of four case studies based on the level of water spilling which are 146 m, 148 m, 150 m and 152 m.

Table 5 displays the six most notable natural frequencies and corresponding mode shapes of the spillway. The first mode take place at 6.3232 Hz with maximum normalised deflection of 0.987, where the side wall at upper part of the spillway is deflected. The deflection is the highest for the spillway. The 2nd, 4th, 14th, 20th and 21st mode occurred at 6.323 Hz, 8.534 Hz, 12.587 Hz, 15.603 Hz and 15.67 Hz respectively. The most significant mode shape with maximum normalised deflection of 0.129 is at the 14th mode with natural frequency of 12.587 Hz that depicted at the upper part of the spillway.

Table 5 - First six natural frequencies and mode shapes of spillway structure

Mode no.	Mode shape	Natural frequency	Normalised deflection
1	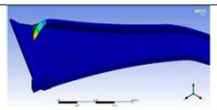	6.323 Hz	0.987
2	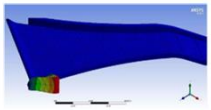	6.418 Hz	0.131
4	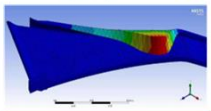	8.534 Hz	0.123
14	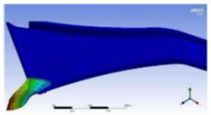	12.587 Hz	0.129
20	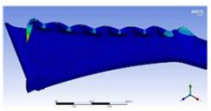	15.603 Hz	0.489
21	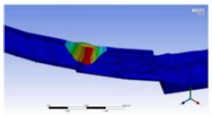	15.67 Hz	0.209

According to the modal analysis, the fourth mode shape of the spillway correlates with the flow of water towards the downstream area, with an associated amplitude value of 8.643 x 10^{-4} m and the natural frequency occurred at 8.534 Hz. Any vibration occurring within this frequency range with a similar mode shape and location must be avoided due to resonance phenomenon. Based on the harmonic response analysis, the greatest deflection occurred in the z-direction with an amplitude value of 1.076 x 10^{-9} m. Table 6 presents the FRF results for the spillway in x, y and z directions. The most significant natural frequency of the x-direction occurred at 6.4 Hz with a maximum deflection of 3.9315 x 10^{-10} m and for y and z-directions, the natural frequency occurred at 12.6 Hz with a maximum deflection of 5.282 x 10^{-11} m and 1.0756 x 10^{-9} m, respectively.

Table 6 - FRF graph for the spillway in x, y and z direction

Direction	FRF graph
x	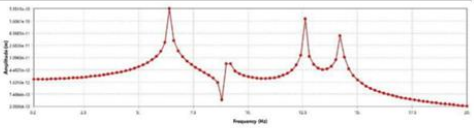
y	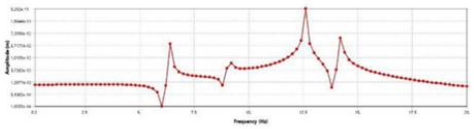
z	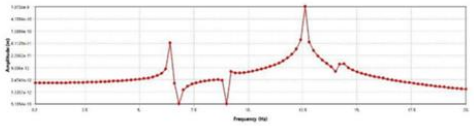

Fig. 36 illustrates the mode shape occurred on the natural frequency of 12.6 Hz and Fig. 37 to Fig. 40 show the ODS occurred on the water level of 146 m, 148 m, 150 m and 152 m, respectively. The correspondence between the mode shape identified in modal analysis and the ODS of FSI analysis at the 146 m water spilling level depicted in Fig. 41 and Fig.42. The transient vibration phenomenon, exhibiting a deflection amplitude of 0.005 m at the operational frequency of 12.549 Hz during this water discharge event, closely aligns with the natural frequency of the spillway which is 12.6 Hz. Thus, the spillway structure experiences significant vibration as a result of this event. However, the locations of induced ODS and mode shape differ for both frequencies. Based on the ODS results, resonance does not occur in the downstream area despite the mode shape being located at the upper spillway. Radzi et. al. conducted a similar investigation in which the resonance phenomena occurred at the Chenderoh Dam intake section due to similar ODS and natural frequency values. Both mode shapes and ODS are most likely comparable due to the high amplitude of the vibration induced in this case [53].

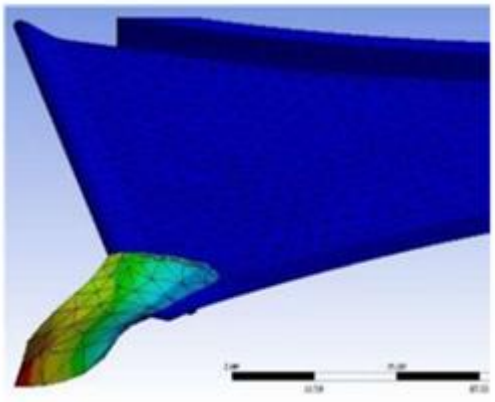

Fig. 36 - Mode shape occurred on the natural frequency

Fig. 37 - Mode shape at 146 m water level

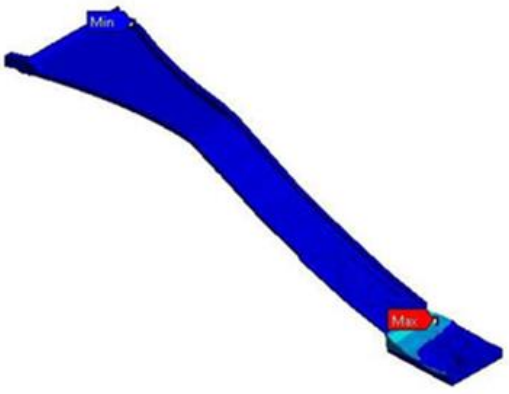

Fig. 38 - Mode shape at 148 m water level

Fig. 39 - Mode shape at 150 m water level

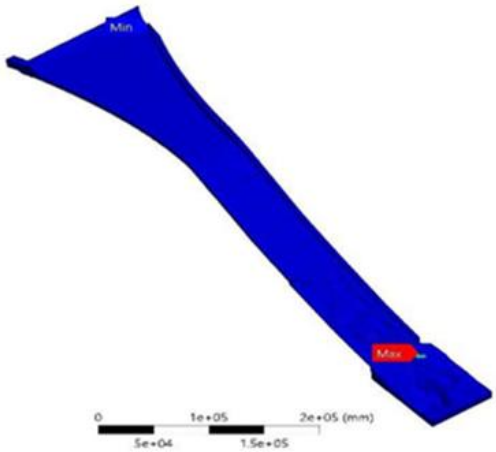

Fig. 40 - Mode shape at 152 m water level

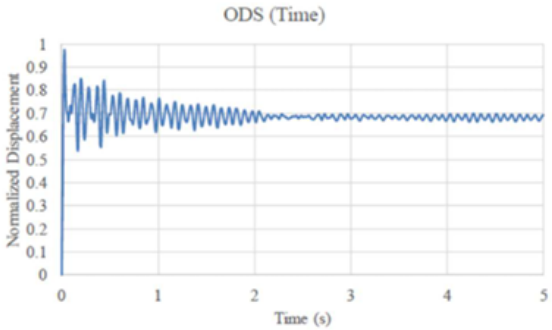

Fig. 41 - Normalised displacement at 146 m water level

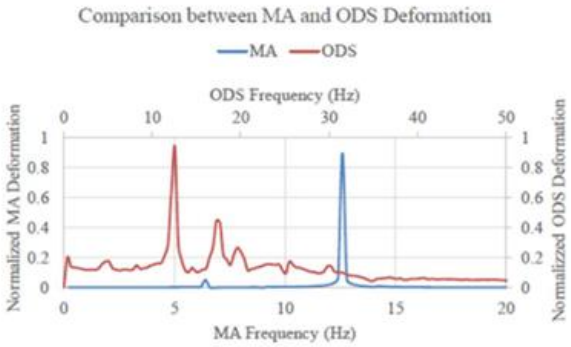

Fig. 42 - Comparison between modal analsysis and ODS deformation at 146 m water level

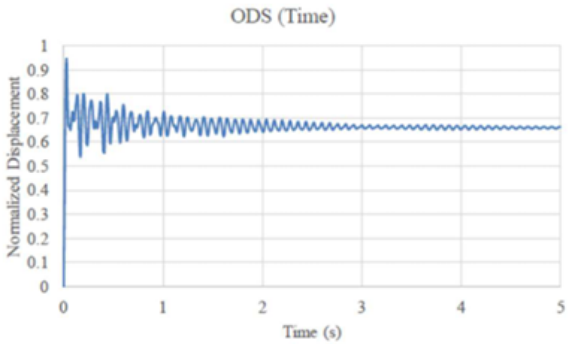

Fig. 43 - Normalised displacement at 146 m water level

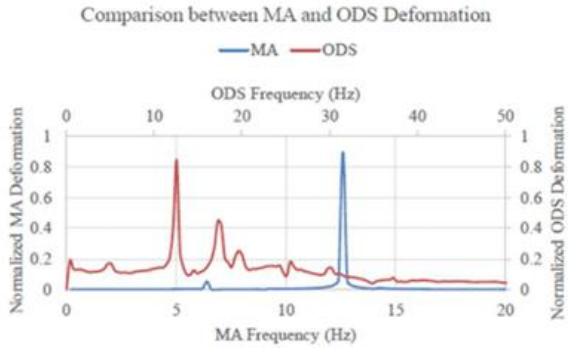

Fig. 44 - Comparison between modal analysis and ODS deformation at 148 m water level

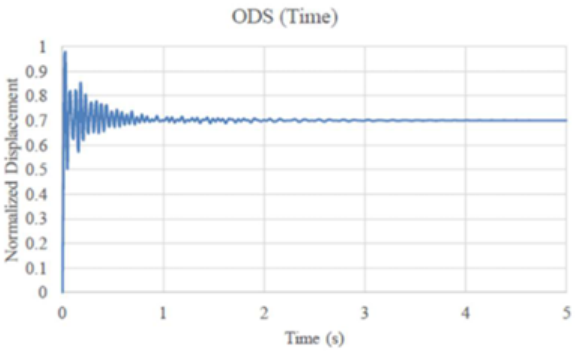

Fig. 45 - Normalised displacement at 150 m water level

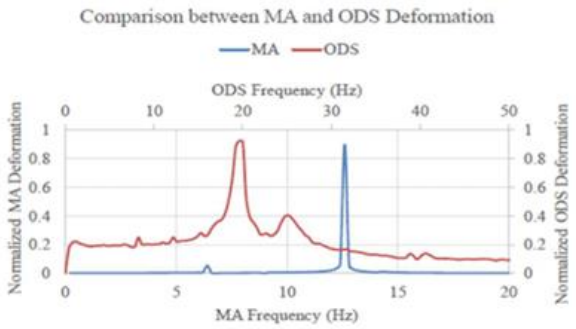

Fig. 46 - Comparison between modal analysis and ODS deformation at 150 m water level

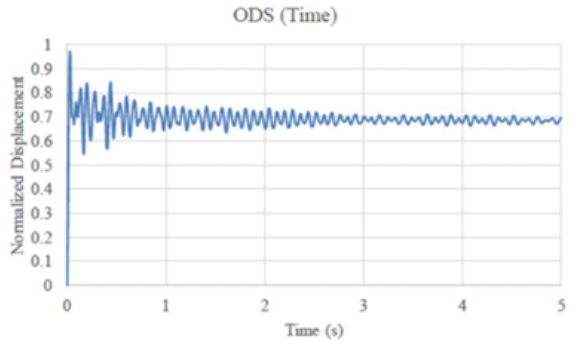

Fig. 47 - Normalised displacement at 152 m water level

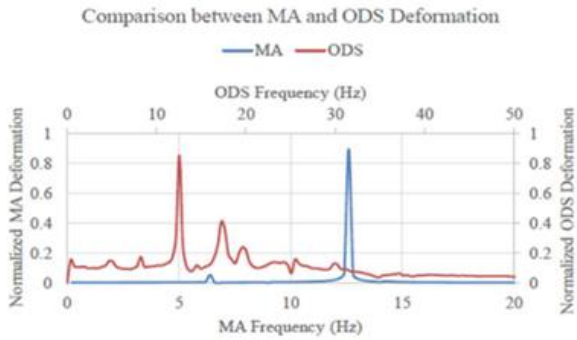

Fig. 48 - Comparison between modal analysis and ODS deformation at 152 m water level

Fig. 43 and Fig. 44 depicted the correspondence between the mode shape identified in modal analysis and the ODS of FSI analysis at the 148 m water spilling level. The transient vibration phenomenon which is exhibiting a deflection amplitude of 0.007 m at the operational frequency of 12.55 Hz during this water discharge event closely aligns with the natural frequency of the spillway which is 12.6 Hz. Thus, the spillway structure experiences significant vibration as a result of this event.

For instance, the Chenderoh Dam sector gate spillway as studied by Radzi et al. [53], experienced resonance due to frequent spilling activities with operational frequencies matching the structure natural modes. Their reported vibration amplitudes and deflections in the intake structure were comparable to the findings at 12.55 Hz and suggest that similar resonance risk zones can occur even in structurally different dam components. However, the locations of induced ODS and mode shape differ for both frequencies. Based on the ODS results, resonance does not occur in the downstream area, despite the mode shape being located at the upper spillway. This is similar to the case of 146 m water level with higher vibration amplitude induced due to more water volume with higher velocity released from the dam.

Fig. 45 and Fig. 46 depicted the correspondence between the mode shape identified in modal analysis and the ODS of FSI analysis at the 150 m water spilling level. The transient vibration phenomenon, exhibiting a deflection amplitude of 0.017 m at the operational frequency of 20 Hz during this water discharge event, closely aligns with the natural frequency of the spillway which is 12.6 Hz. Therefore, both the mode shapes and ODS appeared at different spillway locations no resonance phenomenon occurred. Ghazali et.al. discovered that variable water levels or gate openings for water discharge can cause varied operation frequencies and vibration amplitudes [54]. Resonance is not observed based on the ODS results in the downstream area while the mode shape is at the upper spillway. This is similar to the case of the 148 m water level but with a higher vibration amplitude caused by the high amount of water released at a higher velocity from the dam reservoir. The velocity increased as the water level rose. Therefore, the vibration and deflection of the spillway structure reached the maximum.

Fig. 47 and Fig. 48 depicted the relationship between the mode shape of modal analysis and the ODS of FSI analysis at the 152 m water spilling level. The transient vibration effect with a deflection amplitude value of 0.031 m at the operating frequency of 12.55 Hz during this water spilling is near the natural frequency of the spillway at 12.6 Hz. Thus, the spillway structure experiences significant vibration as a result of this event. However, the locations of induced ODS and mode shape differ for both frequencies.

In 2017, Oroville Dam spillway incident highlighted the destructive potential of uncontrolled flow-induced vibrations which led to severe structural erosion due to cavitation and unattenuated flow turbulence. While the observed maximum vibration amplitude of 0.031 m at Kenyir Dam remains within the elastic limit of the structure. Additionally, guide walls of the Three Gorges and Xiangjiaba dams as noted by Lian et al. [22] were found to suffer fatigue cracking due to prolonged turbulent pressure fluctuations. These walls experienced localized high-frequency vibration with failure risks similar to those observed at Kenyir downstream section although no structural damage has occurred in the cases. This comparison underscores the importance of early vibration detection and reinforcing the importance of periodic condition monitoring even when numerical stress values remain within safe limits.

Table 7 - Vibration risk matrix based on operational and natural frequencies

Parameter	Criteria	Risk Level	Implication
Frequency Proximity	Difference < 1%	High	Possible resonance, increased fatigue risk
	Difference 1–5%	Moderate	Amplified vibration, monitor closely
	Difference > 5%	Low	Unlikely resonance
Vibration Amplitude (Displacement)	> 0.020 m	High	May cause fatigue or long-term damage
	0.010 – 0.020 m	Moderate	Acceptable but should be monitored
	< 0.010 m	Low	Safe
Location of Peak Deflection	Critical structural areas (e.g., joints, anchors)	High	May compromise integrity
	Non-critical areas	Low	Unlikely to affect performance
Material Stress (from harmonic analysis)	> 60% of allowable stress	High	Risk of fatigue accumulation
	30–60% of allowable stress	Moderate	Safe under short-term operation
	< 30% of allowable stress	Low	Within safe limits

A risk-based perspective was introduced by examining the correlation between operational frequencies and natural frequencies to identify potential resonance conditions. Table 7 shows vibration risk matrix based on operational and natural frequencies to translate the vibration analysis results into actionable engineering risk indicators and enhances the engineering decision-support value.

Based on the vibration simulation results, the operational frequency (12.55 Hz) was within 0.4% of the spillway natural frequency (12.6 Hz) which is suggesting a high-risk zone for resonance. However, the locations of the ODS and mode shapes were spatially distinct, particularly between upstream and downstream regions. Thereby, it is mitigating the full resonance risk.

The maximum vibration amplitude recorded which is 0.031 m at 152 m water level falls in the high-risk amplitude range, especially near energy dissipators at the downstream. Despite stress levels being within allowable limits, periodic inspection and condition monitoring are recommended. This risk matrix framework offers a qualitative but practical decision-support tool for identifying critical vibration conditions that may require maintenance intervention or design modification in future study.

3.3 Experimental Validation Results

The validation in terms of water flow velocity has been conducted for both simulation and experimental physical models. As mentioned in methodology, three location points have been selected to measure the velocity using velocity meter which are labelled as Point A, Point B and Point C as depicted in Fig. 7. Point A is located at the spillway inlet, Point B is at the concrete area of spillway prior to granite while Point C is at the granite area of spillway prior to scoured pool or the spillway outlet.

The percentage differences in water flow velocity across all locations at both 2.92 m and 2.96 m water levels are below 10%, generally falling within the acceptable difference range for comparing experimental and simulation studies. Based on these findings, the water flow velocities measured using the velocity meter across all locations demonstrate consistency with the physical model of the Kenyir spillway as outlined in Table 8.

Table 8 - Average velocity along the spillway for different water level

Point	Simulation velocity (m/s)	Experiment velocity (m/s)	Percentage difference (%)
		Water level at 2.92 m	
A	0.885	0.89	0.562
B	2.529	2.55	0.824
C	1.628	1.63	0.123
		Water level at 2.96 m	
A	1.576	1.58	0.253
B	3.123	3.13	0.224
C	2.059	2.06	0.049

Table 9 presents the six most notable natural frequencies and corresponding mode shapes of the spillway. The first mode appears at 969.23 Hz with a maximum normalised deflection of 0.985. The 12th, 17th, 24th, 25th and 30th mode take place at 1984.7 Hz, 2351.9 Hz, 2801.1 Hz, 2853.5 Hz and 3008.6 Hz, respectively. At 24th mode, the mode shape exhibits the highest significance featuring a maximum normalised deflection of 0.155.

Table 9 - First six natural frequencies and mode shapes of physical model spillway

Mode no.	Mode shape	Natural frequency	Normalised deflection
1	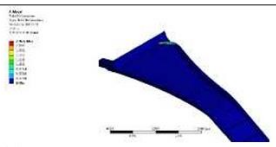	969.23 Hz	0.985
12	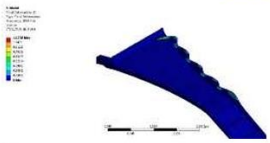	1984.7 Hz	0.489
17	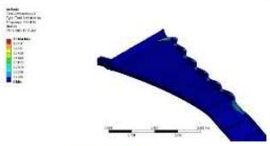	2351.9 Hz	0.484
24	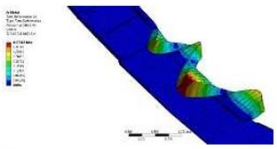	2801.1 Hz	0.155
25	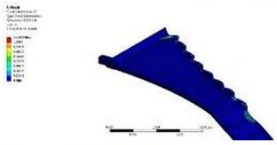	2853.5 Hz	0.501
30	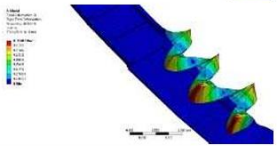	3008.6 Hz	0.147

Table 10 displays the FRF outcomes for the spillway in the x, y, and z directions. The FRF reveal that the most notable natural frequencies in the x, y, and z directions occur at distinct frequencies. For x-direction, the natural frequency occurred 2920 Hz with a maximum deflection of 5.9922 x 10-15 m while for y-direction, the natural frequency take place at 2960 Hz with a maximum deflection of 3.0719 x 10-15 m. For z-direction, the natural frequency occurred at 2840 Hz with maximum deflection of 9.9187 x 10-15 m. The highest deflection was observed in the z-direction for the spillway. According to the modal analysis, the 14th mode shape of the spillway correlates with the water flow towards the downstream area, with an amplitude value of 9.051 x 10-4 m and the natural frequency occurred at 12.6 Hz. It is imperative to prevent any vibration within this frequency range exhibiting a similar mode shape and location to avoid resonance phenomena.

Table 10 - FRF graph for the spillway physical model in x, y and z direction

Direction	FRF graph
x	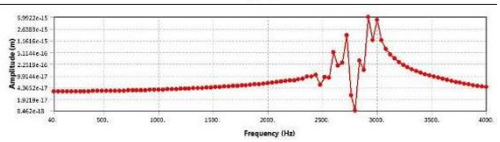
y	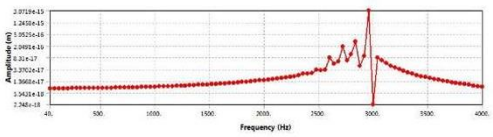
z	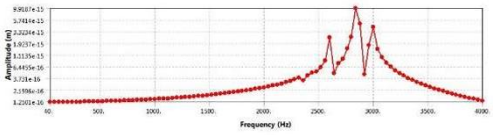

Fig. 49 and Fig. 50 illustrate the correspondence between the mode shape identified in modal analysis and ODS of FSI analysis for the water spilling of 2.92 m which is parallel to water level of 146 m at the real spillway. Despite a transient vibration effect with deflection amplitude value of 5.5 x 10-8 m at the operating frequency of 40.39 Hz during the water spilling level does not coincide with the natural frequency of the spillway at 2801.1 Hz. Therefore, no resonance phenomenon is observed.

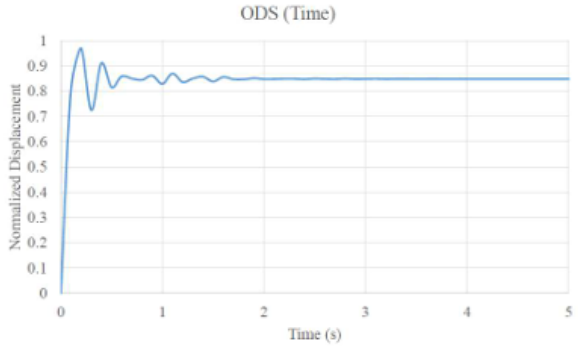

Fig. 49 - Normalised displacement at 2.92 m water level

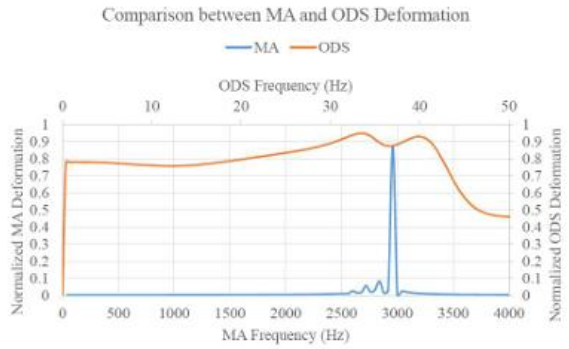

Fig. 50 - Comparison between modal analysis and ODS deformation at 2.92 m water level

Fig. 51 and Fig. 52 illustrates the correlation between the mode shape identified in modal analysis and ODS of FSI analysis for the water spilling of 2.96 m which is parallel to water level of 148 m at the real spillway. Despite a transient vibration effect with a deflection amplitude value of 3.39 x 10-9 m at the operating frequency of 32.94 Hz during the water spilling level does not coincide with the natural frequency of the spillway similarly to water level 2.92 m. Hence, no resonance phenomenon is observed for 2.96 m water level.

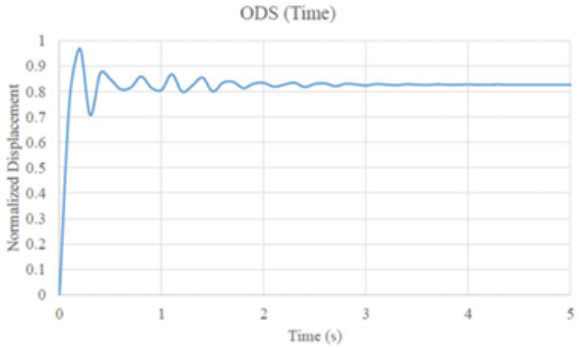

Fig. 51 - Normalised displacement at 2.96 m water level

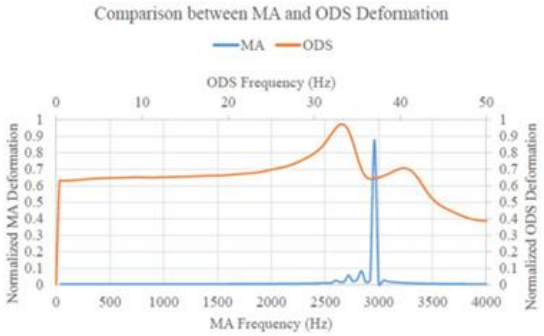

Fig. 52 - Comparison between modal analysis and ODS deformation at 2.96 m water level

Table 11 presents the validation between the numerical and experimental results for the Kenyir Dam spillway physical model. It indicates that there is agreement in the natural frequencies, mode shapes, operating frequency, and ODS between the experiment and simulation. The percentage differences for both simulation and experiment range from 1.345% to 14.01% are below the allowable error percentage for comparing numerical and experimental methods.

Table 11 - EMA and ODS validation between numerical and experimental results

Method	Location	Simulation (Hz)	Experiment (Hz)	Percentage Difference (%)
EMA	Upstream	2853.5	2904.6	1.759
	Downstream	2801.1	2839.3	1.345
ODS	Spillway	40.39	46.97	14.01

4. Conclusion

An increase in velocity and pressure due to rising water levels leads to an acceleration of stress and deformation. The maximum recorded stress and deformation, reaching 2.081 MPa and 0.031 m, respectively, were observed in the granite at the downstream section when the water level reached 152 m. However, this stress remains significantly lower than the allowable maximum compressive strength of granite, which is 49.3 MPa which indicates that the structure remains within safe limits. Nevertheless, incorporation of additional energy dissipators or refinement of aerator placement particularly at Aerator 2 which showed the highest flow velocity and pressure concentration is proposed to reduce the intense

impact pressure that can lead to surface erosion or scouring of the downstream structure especially if the energy is not adequately dissipated. Besides that, design verification against worst-case water levels which is the PMF conditions is advocated to ensure the deformation and stress remain within safe structural limits.

Building upon the previous objective, the most critical mode shape was identified at the 14th mode, with a maximum normalized deflection of 0.129, primarily occurring at the spillway wall. This information is essential for assessing the structural integrity and potential vibration patterns of the spillway, ensuring it can withstand dynamic forces.

Any vibrations occurring within this frequency range, particularly with the same mode shape and location as the 14th mode, must be avoided to prevent resonance. The operational deflection shape (ODS) analysis revealed the highest deflection in the z-direction, with an amplitude of 1.076×10^{-9} m. Additionally, the induced ODS locations and mode shapes differed across all cases, indicating variations in frequency responses. The absence of resonance in the downstream section, despite the mode shape being located at the upper spillway, is crucial for understanding the dynamic behavior of the spillway under operational conditions. However, vibration monitoring systems in critical zones where the operational and natural frequencies show close proximity around 12.6 Hz is suggested to be implemented to support early detection of resonance.

Validation of the numerical simulations using a 1:50 scaled hydraulic physical model further reinforces the credibility of the computational results. The comparison between numerical and experimental flow velocity measurements demonstrated a high degree of accuracy, with a percentage deviation not exceeding 0.824%, confirming the reliability of the numerical data. Furthermore, the validation of numerical vibration analysis showed strong agreement between numerical and experimental results, with a maximum discrepancy of 14.01%. This convergence between computational and physical model data enhances confidence in the findings and contributes to the refinement of analysis methodologies.

In conclusion, this comprehensive study has significantly advanced the understanding of the hydraulic and structural behavior of the Kenyir spillway while also providing practical tools and empirical insights to support future spillway design, operation, and maintenance strategies. The integration of numerical simulations with experimental validation has strengthened the reliability of the findings, making a valuable contribution to dam operations.

Acknowledgement

This research project was supported by Universiti Tenaga Nasional (UNITEN) under the TNB Consultancy grant (U-TG- CR-18- 01).

References

[1] N. H. A. Hassan, K. D. A. Ghani, N. M. Nor, and M. I. F. Rozli, "Structural Damages of Earthfill Dams: A Case study of Teluk Bahang Dam," in AIP Conference Proceedings, American Institute of Physics Inc., Nov. 2022. doi: 10.1063/5.0110061.

[2] R. Faria, S. Oliveira, and A. L. Silvestre, "A Fluid-Structure Interaction Model for Dam Water Systems: Analytical Study and Application to Seismic Behavior," Advances in Mathematical Physics, vol. 2019, 2019, doi: 10.1155/2019/8083906.

[3] K. Saxena and G. Shrivastava, "Study on Overtopping Failure of Concrete DAM: A Review," 2023. [Online]. Available: www.elsevier.com/locate/eng.

[4] F. Salmasi and J. Abraham, "Hydraulic characteristics of flow over stepped and chute spillways (case study: Zirdan Dam)," Water Supply, vol. 23, no. 2, pp. 851–866, Feb. 2023, doi: 10.2166/ws.2023.011.

[5] N. N. Tessema, F. G. Sigtryggsdóttir, L. Lia, and A. K. Jabir, "Case study of dam overtopping fromwaves generated by landslides impinging perpendicular to a reservoir's longitudinal axis," J Mar Sci Eng, vol. 7, no. 7, 2019, doi: 10.3390/jmse7070221.

[6] K. Dong et al., "Analysis of Dam Overtopping Failure Risks Caused by Landslide Induced Surges Considering Spatial Variability of Material Parameters," Front Earth Sci (Lausanne), vol. 9, Jul. 2021, doi: 10.3389/feart.2021.675900.

[7] D. K. H. Ho, K. M. Boyes, and S. M. Donohoo, "Investigation of Spillway Behaviour under Increased Maximum Flood by Computational Fluid Dynamics Technique," 14th Australasian Fluid Mechanics Conference, no. December, pp. 577–580, 2001.

[8] G. Liu, F. Tong, B. Tian, and J. Gong, "Finite element analysis of flood discharge atomization based on water–air two-phase flow," Appl Math Model, vol. 81, pp. 473-486, May 2020, doi: 10.1016/j.apm.2020.01.003.

[9] A. Koskinas et al., "Insights into the Oroville dam 2017 Spillway incident," Geosciences (Switzerland), vol. 9, no. 1, Jan. 2019, doi: 10.3390/geosciences9010037.

[10] J. Lian, Y. Zheng, C. Liang, and B. Ma, "Analysis for the vibration mechanism of the spillway guidewall considering the associated-forced coupled vibration," Applied Sciences (Switzerland), vol. 9, no. 12, 2019, doi: 10.3390/app9122572.

[11] M. P. Paidoussis, "Fluid-Structure Interactions," Fluid-Structure Interactions, pp. 793-10796, 2014, doi: 10.1016/B978-0-12-397312-2.00028-4.

[12] P. Wernberg and P. Davidsson, Fundamentals of Fluid-Structure Interaction Fundamentals of Fluid-Structure Interaction, no. June. 2009. doi: 10.1007/978-3-211-89651-8

[13] E. H. van Brummelen and P. Geuzaine, "Fundamentals of Fluid-Structure Interaction," Encyclopedia of Aerospace Engineering, pp. 1–8, 2010, doi: 10.1002/9780470686652.eae174.

[14] R. Kamakoti and W. Shyy, "Fluid-structure interaction for aeroelastic applications," 2004. doi: 10.1016/j.paerosci.2005.01.001.

[15] Twarog Bernard, "Interaction between hydraulic conditions and structures – fluid structure interaction problem solving. A case study of a hydraulic structure," Technical Transactions, vol. 115, no. 2, pp. 187–209, 2020, doi: 10.4467/2353737xct.18.029.8002.

[16] L. Zhang, G. Yin, S. Wang, and C. Guan, "Study on FSI Analysis Method of a Large Hydropower House and Its Vortex-Induced Vibration Regularities," Advances in Civil Engineering, vol. 2020, 2020, doi: 10.1155/2020/7596080.

[17] B. M. Crookston, A. Anderson, L. Shearin-Feimster, and B. P. Tullis, "Mitigation investigation of flow-induced vibrations at a rehabilitated spillway," ISHS 2014 - Hydraulic Structures and Society - Engineering Challenges and Extremes: Proceedings of the 5th IAHR International Symposium on Hydraulic Structures, no. June, 2014, doi: 10.14264/uql.2014.30.

[18] S. O. Lee, H. Seong, and J. W. Kang, "Flow-induced vibration of a radial gate at various opening heights," Engineering Applications of Computational Fluid Mechanics, vol. 12, no. 1, pp. 567–583, Jan. 2018, doi: 10.1080/19942060.2018.1479662.

[19] K. Riddette and D. Ho, "Assessment of flow-induced vibration in radial gates during extreme flood," 2007.

[20] S. O. Lee, H. Seong, and J. W. Kang, "Flow-induced vibration of a radial gate at various opening heights," Engineering Applications of Computational Fluid Mechanics, vol. 12, no. 1, pp. 567–583, 2018, doi: 10.1080/19942060.2018.1479662.

[21] Y. Zhou, Z. Li, S. Yao, M. Shan, and C. Guo, "Case Study: Influence of Three Gorges Reservoir Impoundment on Hydrological Regime of the Acipenser sinensis Spawning Ground, Yangtze River, China," Front Ecol Evol, vol. 9, Feb. 2021, doi: 10.3389/fevo.2021.624447.

[22] Y. Zhang, J. Lian, S. Li, Y. Zhao, G. Zhang, and Y. Liu, "Predicting dam flood discharge induced ground vibration with modified frequency response function," Water (Switzerland), vol. 13, no. 2, 2021, doi: 10.3390/w13020144.

[23] X. Wang and S. Z. Luo, "Flow-induced vibration study of tunnel spillway working gate on one reservoir," Applied Mechanics and Materials, vol. 226–228, pp. 13–16, 2012, doi: 10.4028/www.scientific.net/AMM.226-228.13.

[24] H. Chanson, "Physical modelling of hydraulics," The Hydraulics of Open Channel Flow, pp. 261–283, 1999, doi: http://dx.doi.org/10.1016/B978-075065978-9/50021-0.

[25] A. El-Zayat, "Physical Modeling For Complex Hydraulic Structures," 2016.

[26] B. J. Heiner and C. C. Shupe, "El Vado Dam – Service Spillway Modification – Physical Model Study Bureau of Reclamation," no. April, 2017.

[27] N. C. Thanh and W. Ling-Ling, "Physical and numerical model of flow through the spillways with a breast wall," KSCE Journal of Civil Engineering, vol. 19, no. 7, pp. 2317–2324, 2015, doi: 10.1007/s12205-015-0742-0.

[28] V. P. Gadhe and S. R. Patnaik, "Physical and Numerical Model Studies of Hirakud Dam Additional Spillway-A Case Study," 9th International Symposium on Hydraulic Structures, vol. 10, no. 5, pp. 1–11, 2022, doi: 10.26077/1bf0-acd4.

[29] Mohd Sidek L, Razali J, Marufuzzaman M, Yalit MR, Radzi MRBM, Hossaian MS. Flood Hydrograph Generation for Kenyir Dam Using Hydrological Modeling System. Water Resources Development and Management 2020;7:64–75, doi.org/10.1007/978 981-15-1971.

[30] Azha SF, Sidek LM, Kok K, Ahmad SA, Saman DH, Allias Omar SM, et al. Assessing dam spillway discharge capacity in response to extreme floods in Perak river hydroelectric scheme: Simulation and proposed mitigation measures. Ain Shams Engineering Journal 2023;14, doi.org/10.1016/j.asej.2023.102540.

[31] M. R. M. Radzi, M. H. Zawawi, L. M. Sidek, M. H. M. Ghazali, and A. Z. A. Mazlan, "Vibration analysis due to frequent spilling over hollow buttress Chenderoh Dam sector gate spillway," Sustainable and Safe Dams Around the World, no. August, pp. 2753-2758, 2019, doi: 10.1201/9780429319778-245.

[32] Numerical simulations of flow discharge and behaviours in spillways Numerical simulations of flow discharge and behaviours in spillways. 2021.

[33] G. Hou, J. Wang, and A. Layton, "Numerical methods for fluid-structure interaction—a review," Commun Comput Phys, vol. 12, no. 2, pp. 337–377, 2012.

[34] A. Bakker, "Lecture 3 - Conservation Equations Applied Computational Fluid Dynamics," 2006.

[35] R. Manikandan and P. Sulthana, "Fluid Structure Interaction (FSI) of Double Curvature Arch Dam Under Seismic Loading By the Application of Added Mass Technique and Acoustic Elements," 2014.

[36] W. Zhang, X. Yang, and J. Wang, "Numerical investigations of dam-break flow impacting on an elastic beam using various FSI coupling algorithms," IOP Conf Ser Mater Sci Eng, vol. 1288, no. 1, p. 012018, Aug. 2023, doi: 10.1088/1757899x/1288/1/012018.

[37] E. E. Alonso and R. Cardoso, "Behavior of materials for earth and rockfill dams: Perspective from unsaturated soil mechanics," Frontiers of Architecture and Civil Engineering in China, vol. 4, no. 1, pp. 1–39, 2010, doi: 10.1007/s11709-010-0013-6.

[38] T. Kishida, D. S. Park, R. L. Sousa, R. Armstrong, and Y. J. Byon, "Modulus reductions of dam embankment materials based on downhole array time series," Earthquake Spectra, vol. 36, no. 1, pp. 400–421, Feb. 2020, doi: 10.1177/8755293019878182.

[39] M. H. Mirabi, H. Akbari, and M. Alembagheri, "Detailed vibrational analysis of unbalanced morning glory spillways using coupled finite volume-finite element method," SN Appl Sci, vol. 3, no. 1, pp. 1–16, 2021, doi: 10.1007/s42452-020-04006-0.

[40] S. Saxena and M. Patel, "Evaluating dynamic behaviour of a concrete dam using modal analysis," Mater Today Proc, vol. 93, pp. 296–301, Jan. 2023, doi: 10.1016/J.MATPR.2023.07.259.

[41] J. Li, T. Bao, and C. E. Ventura, "An automated operational modal analysis algorithm and its application to concrete dams," Mech Syst Signal Process, vol. 168, Apr. 2022, doi: 10.1016/j.ymssp.2021.108707.

[42] Á. Cunha and E. Caetano, "Experimental modal analysis of civil engineering structures," 2006.

[43] M. Azhdary Moghaddam, A. Hasanalipour Shahrabadi, and I. Aminh, "Assessing the Reliability of Cavitation on Chute Spillway by Using Form and Monte Carlo Simulation Method," Irrigation Sciences and Engineering (JISE), vol. 43, no. 3, 2020, doi: 10.22055/jise.2018.23939.1701.

[44] M. C. Aydin, E. Isik, and A. E. Ulu, "Numerical modeling of spillway aerators in highhead dams," Appl Water Sci, vol. 10, no. 1, Jan. 2020, doi: 10.1007/s13201-019-1126-2.

[45] M. C. Aydin, E. Isik, and A. E. Ulu, "Numerical modeling of spillway aerators in high head dams," Appl Water Sci, vol. 10, no. 1, Jan. 2020, doi: 10.1007/s13201-019-1126-2.

[46] M. H. Zawawi et al., "Fluid-structure interactions study on hydraulic structures: A review," in AIP Conference Proceedings, AIP Publishing LLC, 2018, p. 20244.

[47] M. H. Zawawi et al., "Reliability analysis on the reservoir dam spillway structure using fluid-structure interaction," IOP Conf Ser Mater Sci Eng, vol. 920, no. 1, pp. 1–7, 2020, doi: 10.1088/1757-899X/920/1/012030.

[48] R. Faria, S. Oliveira, and A. L. Silvestre, "A Fluid-Structure Interaction Model for Dam Water Systems: Analytical Study and Application to Seismic Behavior," Advances in Mathematical Physics, vol. 2019, 2019, doi: 10.1155/2019/8083906.

[49] H. Asgarzade and A. Memarian, "Nonlinear dynamic analysis of Moshampa Dam Spillway structure and modelling it in finite element software, taking structure soil interaction in to account," 2020. [Online]. Available: www.isca.me

[50] M. H. Zawawi et al., "Fluid-structure interactions study on hydraulic structures: A review," in AIP Conference Proceedings, American Institute of Physics Inc., Nov. 2018. doi: 10.1063/1.5066885.

[51] A. Minmahddun and E. Ngii, "Three dimension deformation analysis of Jatigede Dam," IOP Conf Ser Earth Environ Sci, vol. 419, no. 1, pp. 0–6, 2020, doi: 10.1088/17551315/419/1/012138.

[52] Y. Kim, G. Choi, H. Park, and S. Byeon, "Hydraulic jump and energy dissipation with sluice gate," Water (Switzerland), vol. 7, no. 9, pp. 5115–5133, 2015, doi: 10.3390/w7095115.

[53] Radzi M. R. M., Zawawi M. H., Sidek L. M., Ghazali M. H. M., and Mazlan A. Z. A, "Vibration analysis due to frequent spilling over hollow buttress Chenderoh Dam sector gate spillway," Sustainable and Safe Dams Around the World, pp. 2763–2768, 2019.

[54] M. H. M. Ghazali, A. Z. A. Mazlan, M. A. Azman, M. H. Zawawi, and M. R. M. Radzi, "Flow-Induced Vibration Response of the Chenderoh Dam Bottom Outlet Section Due to the Effects of Water Spilling," IOP Conf Ser Mater Sci Eng, vol. 652, no. 1, pp. 6–12, 2019, doi: 10.1088/1757-899X/652/1/012052.